Boson peak dynamics of natural polymer starch investigated by terahertz time-domain spectroscopy and low-frequency Raman scattering

doi: 10.1016/j.saa.2017.11.051

Boson peak dynamics of natural polymer starch investigated by terahertz time-domain spectroscopy and low-frequency Raman scattering

Wakana Terao[1], Tatsuya Mori*[,1], Yasuhiro Fujii[2], Akitoshi Koreeda[2], Mikitoshi Kabeya[1] and Seiji Kojima[1]

[1]Division of Materials Science, University of Tsukuba, Tsukuba, Ibaraki 305-8573, Japan.
[2]Department of Physical Sciences, Ritsumeikan University, Kusatsu, Shiga 525-8577, Japan.

*Corresponding Author:
Tatsuya Mori (E-mail: mori@ims.tsukuba.ac.jp, Tel: +81-(0)29-853-5304)

Abstract

Terahertz time-domain spectroscopy and low-frequency Raman scattering were performed on the natural polymer starch to investigate the boson peak (BP) dynamics. In the infrared spectrum, the BP was observed at 0.99 THz at the lowest temperature. Compared to the result from a previous study for vitreous glucose, both the frequency of the BP and absorption coefficient show lower values than those of the vitreous glucose. These behaviors originate from the longer correlation length of the medium-range order and lower concentration of hydroxyl groups in the starch. In the Raman spectrum, the BP was observed at 1.1 THz at room temperature, although the BP was not observed around room temperature due to the excess wing of the fast relaxation modes in the infrared spectrum. The temperature dependence of $\varepsilon''(\nu)$ during the heating process and cooling process shows a hysteresis below 230 K. During the heating process, kinks were observed at 140 K and 230 K. These kinks are attributed to the β-relaxation and the β_{wet}-relaxation, respectively.

Keywords:

Boson peak, Terahertz time-domain spectroscopy, Low-frequency Raman scattering, Starch, Amorphous.

Introduction

In the terahertz (THz) region, a low energy excitation called the boson peak (BP) is universally observed in materials having an amorphous structure [1,2], and the BP dynamics is one of the unresolved problems of glass physics. To elucidate the origin of the BP, significant number of experimental [2-15] and theoretical [16-24] studies has been done over the past several decades. The BP is regarded as the excess vibrational density of states (VDOS) $g(\nu)$ [1], and appears as a peak in the $g(\nu)/\nu^2$ spectrum. The BP is detectable by inelastic neutron [3-7] or X-ray [8,9] scattering, low-frequency Raman scattering [10-12], and low-temperature specific heat [2,13,14]. The BP is also detectable by terahertz-time-domain spectroscopy (THz-TDS); i.e., far infrared (IR) spectroscopy [25-34], which is not well known. However, recently, THz-TDS is becoming recognized as suitable for the detection of the BP [34]. In order to understand how to detect the BP by THz-TDS, it is necessary to consider the relational expression $\alpha(\nu) = C_{\mathrm{IR}}(\nu) \cdot g(\nu)$ derived from the linear response theory for amorphous materials [35-38]. The BP appears in the $g(\nu)/\nu^2$ spectrum, therefore it is expected that the BP in the IR spectrum appears in the $\alpha(\nu)/\nu^2$ spectrum. Actually, the BP of vitreous glucose has been clearly detected in a previous study by THz-TDS [34].

Starch is a natural polymer formed by the polymerization of a number of D-glucose molecules by glycosidic linkages, and includes two polymers amylose and amylopectin [39-42]. By detecting the BP of starch, we can discuss the change in the BP dynamics between a monomer and polymer by comparison with the BP of glucose [34]. In a common type of starch, the relative weight percent of amylose and amylopectin is about 80 % amylopectin and 20 % amylose [40]. It is known that the content of both amylose and amylopectin is changed depending on the plant from which it is derived, which affects the crystallinity and temperature of the glass transition; T_g. The study of the X-ray powder diffraction of starch [39] indicated that the degree of the crystallinity of starch decreases as the amylose content increases. The T_g of starch also depends on the moisture content [43], and the starch which has the same origin, the higher the water content, the lower the T_g [44,45]. Previous studies [43-49] of the T_g of starch by differential scanning calorimetry (DSC) measurements of the various types and the moisture content of starch have been performed, and the T_g of the starch measured by these studies showed the range of approximately 278 K [47] to 400 K [46]. Based on the dielectric spectroscopy of amylo-maise-starch [50], the δ-relaxation, β-relaxation, and β_{wet}-relaxation have been observed. These relaxations observed in the dielectric spectrum show the different temperature dependence, and a shift to a higher frequency as the temperature increases. According to the study of the relaxation of polyhydric

alcohol by THz-TDS [51,52], the bend points of the temperature dependence of the complex dielectric constant at the BP frequency correspond to the freezing temperature of relaxation modes.

In this study, we performed the THz-TDS on starch, and we detected the BP in the $\alpha(\nu)/\nu^2$ spectrum. As a complementary spectroscopic method, we also performed low-frequency Raman scattering spectroscopy. We compared the results of the starch with the BP frequency and the absolute values of the absorption coefficient of glucose glass from a previous study [34]. We also compare the contribution of the excess wing with the result of the previous study of the dielectric measurement [50], and find that the dielectric response in the THz region has relevance to the fast relaxation modes.

Experimental

The powdered soluble starch was purchased from Wako Pure Chemical Industries, Ltd. The measured sample was a disk-shaped pellet with a diameter of about 15 mm and a thickness of 1.457 mm.

The THz-TDS (RT-10000, Tochigi Nikon Co.) with low-temperature-grown GaAs photoconductive antennas for both the emitter and detector (Hamamatsu Photonics KK), covering the frequency range of 0.25–2.25 THz, was carried out using the standard transmission configuration for the temperature-dependent measurements. The temperature was varied from 33 to 300 K using a liquid-helium flow cryostat system (Helitran LT-3B, Advanced Research Systems) [34,53,54].

Confocal micro-Raman measurements were performed with a depolarized backscattering geometry [55]. A frequency-doubled diode-pumped solid-state (DPSS) Nd:yttrium-aluminum-garnet laser oscillating in a single longitudinal mode at 532 nm (Oxxius LMX-300S) was employed as the excitation source. A home-built microscope with ultranarrow-band notch filters (OptiGrate) was used to focus the excitation laser and collect the Raman-scattered light. The scattered light was analyzed by a single monochromator (Jovin-Yvon, HR320, 1200 grooves/mm) equipped with a charge-coupled device (CCD) camera (Andor, DU420).

Results and Discussion

Figure 1 shows the temperature dependence of both (a) the real $\varepsilon'(\nu)$ and (b) imaginary $\varepsilon''(\nu)$ parts of the complex dielectric constant of starch during the heating process obtained by THz-TDS. As the temperature increases, the values of both the real and imaginary parts of the ε increase. At 33 K, in the real part $\varepsilon'(\nu)$, a clear peak is observed around 0.7 THz. This peak becomes broad as the temperature increases and it

disappears above about 180 K. On the other hand, the imaginary part $\varepsilon''(\nu)$ shows an inflection point around 0.7 THz at the low temperature. The frequencies of the inflection point and the peak of the real part $\varepsilon'(\nu)$ are almost identical, which is attributed to the relation between real and imaginary parts of the response function. The spectrum consists of a superposition of the VDOS peak and excess wings of the fast relaxation modes, and the temperature change is mainly caused by the latter contribution.

Figure 2 shows the temperature dependence of the $\alpha(\nu)/\nu^2$ spectrum, which is the representation of the BP in the IR spectrum. At the lowest temperature of 33 K, the BP is observed at 0.99 THz. As the temperature increases, the spectral shape of the BP broadens and the peak position slightly shifts toward a lower frequency. Furthermore, the BP disappears above 180 K and the behavior is similar to that of the $\varepsilon'(\nu)$. The broadening and disappearance of the BP are due to the excess wing of the relaxation modes which shifts toward the higher frequency as the temperature increases; i.e., the disappearance does not mean that the BP has intrinsically disappeared. Generally, the contribution of the relaxation mode is strong in the fragile system [56], and it partially hides the BP structure. This situation is well known in the Raman experiments [56,57]. The VDOS structure should be analyzed without the contribution of the relaxation mode. However, it is difficult to subtract the contribution of the relaxation mode from the experimental spectrum because the structure of the excess wing itself is under debate [58]. We only point out that the frequency dependence of the excess wing of the starch seems to decrease slightly toward higher frequencies in the measured frequency range.

For comparison of the BPs of starch and vitreous glucose obtained by the previous study [34], the $\alpha(\nu)/\nu^2$ spectra of starch and vitreous glucose at a low temperature are shown in Fig. 3. The BP frequency and the BP intensity of starch are about 10 % and about 30 % lower than those of vitreous glucose [34], respectively. Regarding the lowering of the BP frequency, it indicates an increase in the correlation length of the medium-range order, when we assume that the transverse sound velocity has not changed. Therefore, assuming that the transverse sound velocities of the starch and vitreous glucose are the same values, the 10 % lowering of the BP frequency indicates a 10 % increase in the correlation length of the medium-range order. As a general feature, the polymer has a longer correlation length of the medium-range order compared to the monomer, thus our obtained results are reasonable.

We then considered the reason why the BP intensity of the starch is lower than that of the vitreous glucose. The ratio of the absorption coefficient of starch to vitreous glucose around 1 THz is about 0.7. The number of hydroxyl groups (OH) contained per structural unit of the monomer is 3 for starch [59] and 5 for glucose [60,61], and their

ratio is 0.6, which is close to the value of the ratio of the absorption coefficient around 1 THz. Assuming that the IR absorption in the vicinity of the BP frequency originates from the randomly oriented OH groups, it might be expected that the absorption coefficient of starch is proportional to the number of OH groups per unit volume. Similar tendency has also been observed in previous studies of polyhydric alcohols [33].

To investigate the contribution of the fast relaxation modes in the complex dielectric constant spectrum around the BP frequency, we discuss the temperature dependence of the imaginary part $\varepsilon''(\nu)$ at 1 THz during both the cooling and heating processes ($\varepsilon''_{\mathrm{cool}}$(1 THz, T) and $\varepsilon''_{\mathrm{heat}}$(1 THz, T)) which are shown in Fig. 4(a). During the cooling process, the value of $\varepsilon''_{\mathrm{cool}}$(1 THz, T) almost monotonically decreases. On the other hand, during the heating process, the bend points are observed at 140 K and 230 K, in the $\varepsilon''_{\mathrm{heat}}$(1 THz, T); i.e., the complex dielectric constants of the starch shows a clear thermal hysteresis below 230 K. A similar behavior is observed in protein [62] and other glasses [63]. According to a previous study of natural polymer amber [63], this behavior is attributed to the existence of water in very small spaces of the starch.

Figure 4(c) shows the temperature dependence of the relaxation times [50] of the β-relaxation and β_{wet}-relaxation modes ($\tau_{\beta}(T)$ and $\tau_{\beta\mathrm{wet}}(T)$) of the starch obtained from dielectric spectroscopy which has been done by Einfeldt *et al*. [50]. According to another measurement of the dielectric constant of cellulose [64], these relaxations are assigned such that β_{wet}-relaxation corresponds to the motion of the water–polymer complexes and the β-relaxation corresponds to the local chain motion. Although the bend points are not observed in both the $\tau_{\beta}(T)$ and the $\tau_{\beta\mathrm{wet}}(T)$, the two bend points observed in the $\varepsilon''_{\mathrm{heat}}$(1 THz, T) coincide with the temperature at which the $\tau_{\beta}(T)$ and the $\tau_{\beta\mathrm{wet}}(T)$ reach almost 100 seconds, respectively. Therefore, the temperatures of the bend points in the $\varepsilon''_{\mathrm{heat}}$(1 THz, T) of starch at 140 K and 230 K will correspond to the freezing temperatures of the β-relaxation and β_{wet}-relaxation modes, respectively.

Figure 4(b) shows the temperature dependence of the BP frequency. The value of the BP frequency is obtained by fitting the $\alpha(\nu)/\nu^2$ spectrum of Fig. 2 with a polynomial.

During the cooling process, a broad peak like a plateau first appears from 180 K, and the BP frequency monotonically increases toward the lower temperature. On the other hand, during heating process, the temperature dependence of the BP frequency shows a behavior inverse of the temperature dependence of $\varepsilon''_{\mathrm{heat}}$(1 THz, T), and the BP vanishes above 250 K in the $\alpha(\nu)/\nu^2$ spectrum. The disappearance of the BP in the $\alpha(\nu)/\nu^2$ spectrum is mainly caused by the increase in the contribution of the excess wing of the fast relaxation modes at the higher temperature, and it does not mean intrinsic softening of the BP at the high temperature.

Finally, we investigated the behavior of the BP by the low-frequency Raman scattering and compared the results to that of the THz-TDS. Figure 5(a) shows the Raman intensity spectra I_{exp} at room temperature and Fig. 5(b) shows the imaginary part of the Raman susceptibility $\chi''(\nu)$ and the $\chi''(\nu)/\nu$ spectrum which are evaluated from I_{exp} using the following equation [65,66]:

$$\chi''(\nu) = \frac{I_{\mathrm{exp}}(\nu)}{n_{\mathrm{B}}(\nu, T) + 1}, \quad (1)$$

where $n_{\mathrm{B}}(\nu) = [\exp(h\nu/k_{\mathrm{B}}T) - 1]^{-1}$ is the Bose-Einstein distribution function. The BP in the Raman spectrum is discussed by the following equation [67]:

$$\nu \cdot \chi''(\nu) = C_{\mathrm{Raman}}(\nu) \cdot g(\nu), \quad (2)$$

where $C_{\mathrm{Raman}}(\nu)$ is the Raman light-vibration coupling coefficient. The $\chi''(\nu)/\nu$ spectrum corresponds to the $\alpha(\nu)/\nu^2$ spectrum; i.e., $\chi''(\nu)/\nu$ is the BP representation of the Raman spectrum. The difference of the BP frequencies between IR and Raman spectrum can be attributed to the different frequency dependences between $C_{\mathrm{IR}}(\nu)$ and $C_{\mathrm{Raman}}(\nu)$ in the vicinity of the BP frequencies.

In the spectrum of $\chi''(\nu)/\nu$, the BP is clearly observed and the BP frequency of the Raman spectrum ($\nu_{\mathrm{BP\text{-}Raman}}$) is about 1.1 THz. I_{exp} also shows a peak around $\nu_{\mathrm{BP\text{-}Raman}}$, which is an universal artifact due to the high temperature approximation for the thermal factor ($n_{\mathrm{B}} + 1$) [34]. The BP is not observed in the $\alpha(\nu)/\nu^2$ above about 250 K due to the effect of the excess wing but it is clearly observed in the $\chi''(\nu)/\nu$ spectrum even at room temperature. This behavior suggests that the fast relaxation modes of starch are more IR active than Raman active. It will be important to compare the behaviors of the BP of both IR and Raman spectra at the low temperature where the motion of fast modes has frozen, which is a future study.

Conclusion

THz-TDS and low-frequency Raman scattering were performed on the natural polymer starch to investigate the BP dynamics. In the IR spectrum, the BP was clearly observed at 0.99 THz at the lowest temperature of 33 K. Comparing the result of starch to that of vitreous glucose from a previous study [34], both the frequency of the BP and absorption coefficient showed 10 % and 30 % lower values, respectively, than those of the vitreous glucose. These behaviors are attributed to the longer correlation length of the medium-range order and lower concentration of hydroxyl groups in the starch. In the Raman spectrum, the BP was observed at 1.1 THz at room temperature. On the other hand, the BP was not observed around room temperature due to the excess wing of the fast relaxation modes. The temperature dependence of ε'' during the heating process and

cooling process showed a hysteresis below 230 K. A similar hysteresis has been observed in protein [62] and other glasses [63]. During the heating process, kinks were observed at 140 K and 230 K. These temperatures were in good agreement with the freezing temperatures [50] of the β-relaxation and the β_{wet}-relaxation, respectively.

ACKNOWLEDGMENTS

The authors are grateful to Y. Matsuda for the crucial idea and advice about the BP detection by THz-TDS. This work was partially supported by JSPS KAKENHI Grants No. 17K14318 and No. 26287067, the Nippon Sheet Glass Foundation for Materials Science and Engineering, the Murata Science Foundation, and the Asahi Glass Foundation.

References

[1] T. Nakayama, Rep. Prog. Phys., 65 (2002) 1195.

[2] W. A. Phillips, *Amorphous Solids: Low-Temperature Properties* (Springer, Berlin, 1981).

[3] U. Buchenau, M. Prager, N. Nücker, A. J. Dianoux, N. Ahmad, W. A. Phillips, Phys. Rev. B, 34 (1986) 5665.

[4] O. Yamamuro, K. Harabe, T. Matsuo, K. Takeda, I. Tsukushi, T. Kanaya, J. Phys. Condens. Matter, 12 (2000) 5143.

[5] M. Nakamura, M. Arai, T. Otomo, Y. Inamura, S. M. Bennington, J. Non-Cryst. Solids, 293-295 (2001) 377.

[6] N. Violini, A. Orecchini, A. Paciaroni, C. Petrillo, F. Sacchetti, Phys. Rev. B, 85 (2012) 134204.

[7] M. Zanatta, A. Fontana, A. Orecchini, C. Petrillo, F. Sacchetti, J. Phys. Chem. Lett., 4 (2013) 1143.

[8] G. Baldi, V. M. Giordano, G. Monaco, B. Ruta, Phys. Rev. Lett., 104 (2010) 195501.

[9] B. Ruta, G. Baldi, F. Scarponi, D. Fioretto, V. M. Giordano, G. Monaco, J. Chem. Phys., 137 (2012) 214502.

[10] V. K. Malinovsky, A. P. Sokolov, Solid State Commun., 57 (1986) 757.

[11] S. Kojima, Phys. Rev. B, 47 (1993) 2924.

[12] N. V. Surovtsev, A. P. Sokolov, Phys. Rev. B, 66 (2002) 054205.

[13] R. C. Zeller, R. O. Pohl, Phys. Rev. B, 4 (1971) 2029.

[14] G. Baldi, G. Carini Jr., G. Carini, A. Chumakov, R. D. Maschio, G. D'Angelo, A. Fontana, E. Gilioli, G. Monaco, L. Orsingher, B. Rossi, M. Zanatta, Philos. Mag., 96 (2016) 754.

[15] A. I. Chumakov, G. Monaco, A. Monaco, W. A. Crichton, A. Bosak, R. Rüffer, A. Meyer, F. Kargl, L. Comez, D. Fioretto, H. Giefers, S. Roitsch, G. Wortmann, M. H. Manghnani, A. Hushur, Q. Williams, J. Balogh, K. Parliński, P. Jochym, P. Piekarz, Phys. Rev. Lett., 106 (2011) 225501.

[16] T. S. Grigera, V. Mart´ın-Mayor, G. Parisi, P. Verrocchio, Nature (London), 422 (2003) 289.

[17] W. Götze, M. R. Mayr, Phys. Rev. E, 61 (2000) 587.

[18] D. A. Parshin, Phys. Scr., T49A (1993) 180.

[19] E. Duval, A. Boukenter, T. Achibat, J. Phys. Condens. Matter, 2 (1990) 10227.

[20] T. Nakayama, Phys. Rev. Lett., 80 (1998) 1244.

[21] M. I. Klinger, A. M. Kosevich, Phys. Lett. A, 280 (2001) 365.

[22] W. Schirmacher, G. Diezemann, C. Ganter, Phys. Rev. Lett., 81 (1998) 136.
[23] S. N. Taraskin, Y. L. Loh, G. Natarajan, S. R. Elliott, Phys. Rev. Lett., 86 (2001) 1255.
[24] H. Mizuno, S. Mossa, J. L. Barrat, Europhys. Lett., 104 (2013) 56001.
[25] K. Matsuishi, S. Onari, T. Arai, Jpn. J. Appl. Phys., 25 (1986) 1144.
[26] K. W. Hutt, W. A. Phillips, R. J. Butcher, J. Phys. Condens. Matter, 1 (1989) 4767.
[27] T. Ohsaka, T. Ihara, Phys. Rev. B, 50 (1994) 9569.
[28] T. Ohsaka, S. Oshikawa, Phys. Rev. B, 57 (1998) 4995.
[29] M. Naftaly, R. E. Miles, J. Non-Cryst. Solids, 351 (2005) 3341.
[30] S. Kojima, T. Mori, T. Shibata, Y. Kobayashi, Pharm. Anal. Acta, 6 (2015) 401.
[31] T. Shibata, T. Mori, S. Kojima, Spectrochim. Acta A, 150 (2015) 207.
[32] J. Sibik, J. A. Zeitler, Philos. Mag., 96 (2015) 842.
[33] S. Koda, T. Mori, S. Kojima, J. Mol. Struct., 1126 (2016) 127.
[34] M. Kabeya, T. Mori, Y. Fujii, A. Koreeda, B. W. Lee, J. H. Ko, S. Kojima, Phys. Rev. B, 94 (2016) 224204.
[35] F. L. Galeener, P. N. Sen, Phys. Rev. B, 17 (1978) 1928.
[36] S. N. Taraskin, S. I. Simdyankin, S. R. Elliott, J. R. Neilson, T. Lo, Phys. Rev. Lett., 97 (2006) 055504.
[37] S. N. Taraskin, J. Phys. Condens. Matter, 19 (2007) 415113.
[38] S. N. Taraskin, S. I. Simdyankin, S. R. Elliott, J. Phys. Condens. Matter, 19 (2007) 455216.
[39] N. W. H. Cheetham, L. Tao, Carbohyd. Polym., 36 (1998) 277.
[40] A. Buléon, P. Colonna, V. Planchot, S. Ball, Int. J. Biol. Macromal., 23 (1998) 85.
[41] P. J. Jenkins, A. M. Donald, Int. J. Biol. Macromol., 17 (1995) 315.
[42] U. Trommsdorff, I. Tomka, Macromolecules, 28 (1995) 6128.
[43] P. Liu, L. Yu, H. Liu, L. Chen, L. Li, Carbohyd. Polym., 77 (2009) 250.
[44] K. J. Zeleznak, R. C. Hoseney, Cereal. Chem., 64(2) (1987) 121.
[45] Å. Rindlav, S. H. D. Hullernan, P. Gatenholm, Carbohyd. Polym., 34 (1997) 27.
[46] R.J. Nicholls, I. A. M. Appelqvist, A. P. Davies, S.J. Ingman, P. J. Lillford, J. Cereal. Sci., 21 (1995) 25.
[47] J. J. G. van Soest, K. Benes, D. de Wit, J. F. G. Vliegenthart, Polymer, 37 (1996) 3543.
[48] A. Mizuno, M. Mitsuiki, M. Motoki, J. Agr. Food. Chem., 46 (1998) 98.
[49] W. Bindzus, S. J. Livings, H. G. Hernandez, G. Fayard, B. van. Lengerich, F. Meuser, Starch-Starke, 54 (2002) 393.
[50] J. Einfeldt, D. Meißner, A. Kwasniewski, L. Einfeldt, Polymer., 42 (2001) 7058.

[51] J. Sibik, S. R. Elliott, J. A. Zeitler, J. Phys. Chem. Lett., 5 (2014) 1968.
[52] E. P. J. Parrott, J. A. Zeitler, Appl. Spectrosc., 69 (2015) 1.
[53] T. Mori, H. Igawa, S. Kojima, IOP Conf. Ser.: Mater. Sci. Eng., 54 (2014) 012006.
[54] M. A. Helal, T. Mori, S. Kojima, Appl. Phys. Lett., 106 (2015) 182904.
[55] Y. Fujii, D. Katayama, A. Koreeda, Jpn. J. Appl. Phys., 55 (2016) 10TC03.
[56] A. P. Sokolov, E. Rössler, A. Kisliuk, D. Quitmann, Phys. Rev. Lett., 71 (1993) 2062.
[57] A. Hédoux, Y. Guinet, M. Descamps, Phys. Rev. B, 58 (1998) 31.
[58] K. L. Ngai, S. Capaccioli, D. Prevosto, L. M. Wang, J. Phys. Chem. B, 119 (2015) 12519.
[59] O. L. Sponsler, J. Gen. Physiol., 5 (1923) 757.
[60] G. M. Brown, H. A. Levy, Acta Crystallogr., Sect. B, 35 (1979) 656.
[61] S. C. Chu, G. A. Jeffrey, Acta Crystallogr., Sect. B, 24 (1968) 830.
[62] N. Yamamoto, K. Ohta, A. Tamura, K. Tominaga, J. Phys. Chem. B, 120 (2016) 4743.
[63] T. Sasaki, Y. Hashimoto, T. Mori, S. Kojima, Int. Lett. Chem. Phys. Astron., 65 (2015) 29.
[64] J. Einfeldt, D. Meißner, A. Kwasniewski, Cellulose, 11 (2004) 145.
[65] W. Hayes, R. Loudon, *Scattering of Light by Crystals* (Wiley, New York, 1978).
[66] S. N. Yannopoulos, K. S. Andrikopoulos, G. Ruocco, J. Non-Cryst. Solids, 352 (2006) 4541.
[67] R. Shuker, R. W. Gammon, Phys. Rev. Lett., 25 (1970) 222.

Figure captions

Figure 1. Temperature dependence of (a) the real $\varepsilon'(\nu)$ and (b) imaginary parts $\varepsilon''(\nu)$ of complex dielectric constants of the starch during the heating process at 33, 40, . . . , 300 K. The data are plotted every 10 K above 40 K.

Figure. 2. Temperature dependence of the BP plot $\alpha(\nu)/\nu^2$ of the starch during the heating process, at 33, 40, . . . , 300 K. The data are plotted every 10 K above 40 K.

Figure. 3. Comparison of the BP plot $\alpha(\nu)/\nu^2$ of the starch at 33 K and the vitreous glucose at 14 K.

Figure. 4. (a) Temperature dependence of the imaginary part of the complex dielectric constant $\varepsilon''(\nu)$ at 1 THz of the starch during the heating process and the cooling process. (b) Temperature dependence of the BP frequency of the IR spectrum during the heating process and the cooling process. The star plot shows the BP frequency of the Raman spectrum at room temperature.
(c) The temperature dependence of the relaxation times of the β-relaxation and β_{wet}-relaxation modes ($\tau_\beta(T)$ and $\tau_{\beta\mathrm{wet}}(T)$) obtained from the dielectric spectroscopy which has been done by Einfeldt *et al*. [50]. The vertical grid lines are drawn at 140 K and 230 K and the horizontal line is drawn at the relaxation time of 100 seconds.

Figure. 5. (a) Raman intensity spectra of the starch at room temperature. (b) The orange spectra are the imaginary part of the Raman susceptibility $\chi''(\nu)$ and the green spectra are the $\chi''(\nu)/\nu$ spectra.

Figure. 1.

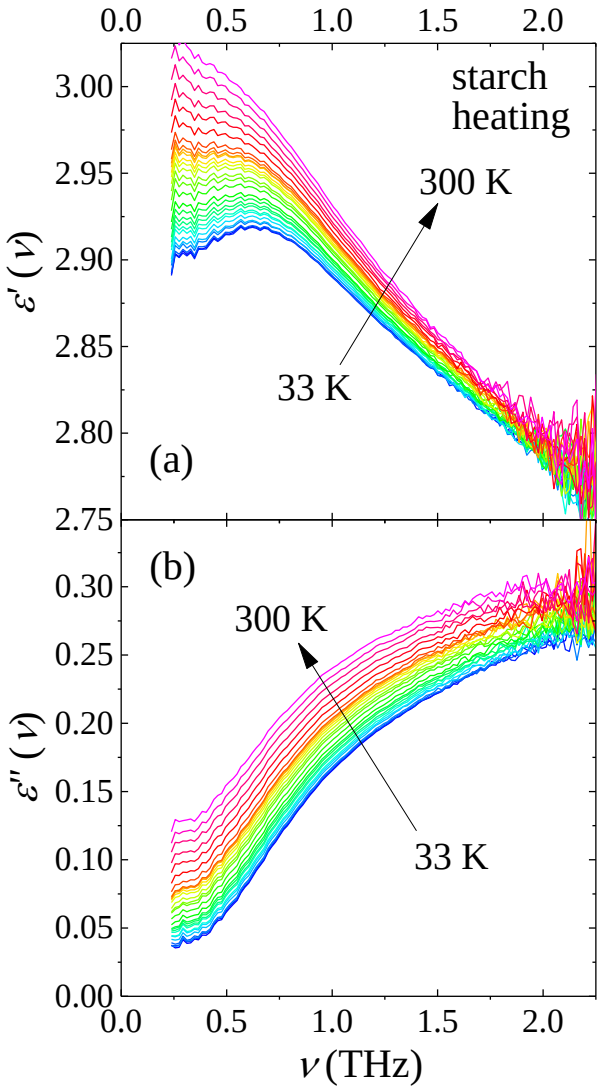
starch
heating
300 K
33 K
(a)
(b)
300 K
33 K
ε' (ν)
ε'' (ν)
ν (THz)
0.0
0.5
1.0
1.5
2.0
3.00
2.95
2.90
2.85
2.80
2.75
0.30
0.25
0.20
0.15
0.10
0.05
0.00

Figure. 2.

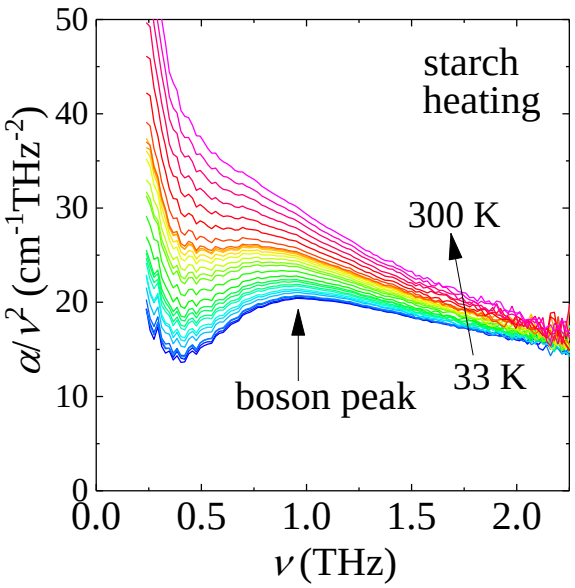
starch
heating
300 K
33 K
boson peak
α/ν^2 (cm^{-1}THz^{-2})
ν (THz)
0
10
20
30
40
50
0.0
0.5
1.0
1.5
2.0

Figure. 3.

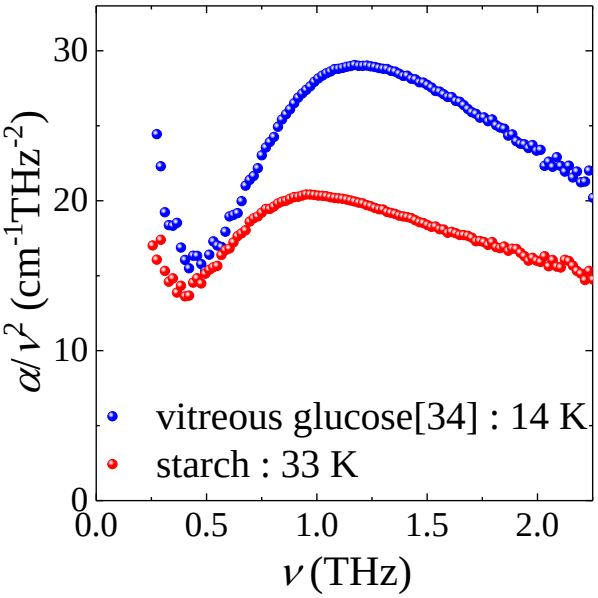
30
20
10
0
0.0
0.5
1.0
1.5
2.0
α/ν^2 (cm^{-1}THz^{-2})
ν (THz)
vitreous glucose[34] : 14 K
starch : 33 K

Figure. 4.

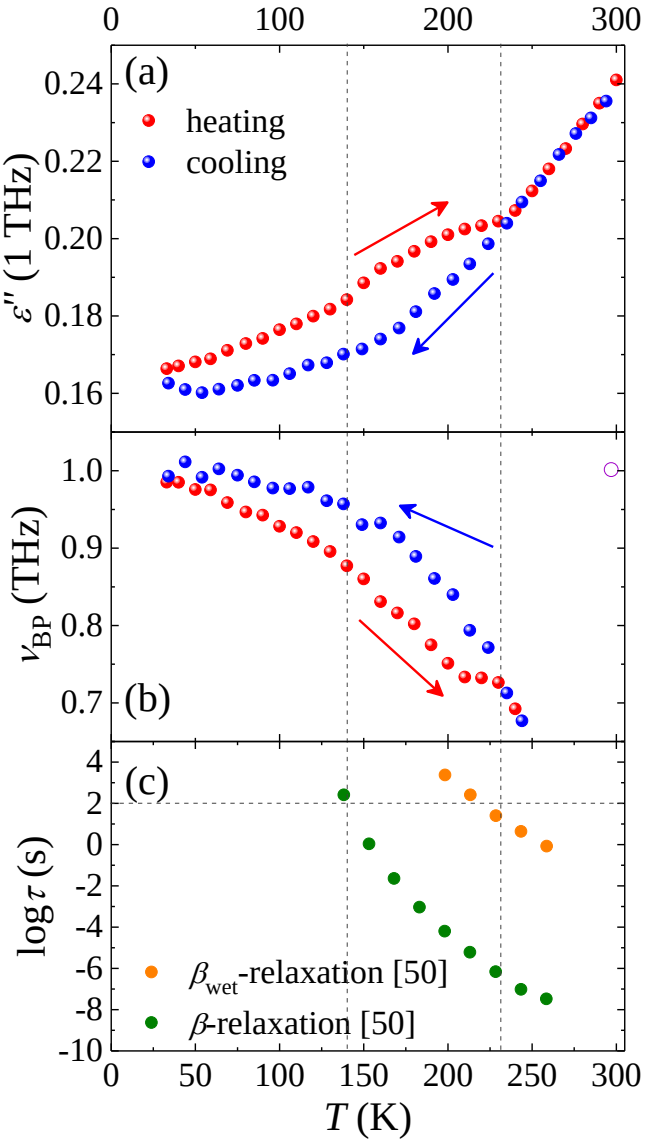
(a)
heating
cooling
ε'' (1 THz)
(b)
ν_BP (THz)
(c)
log τ (s)
β_wet-relaxation [50]
β-relaxation [50]
T (K)

Figure. 5.

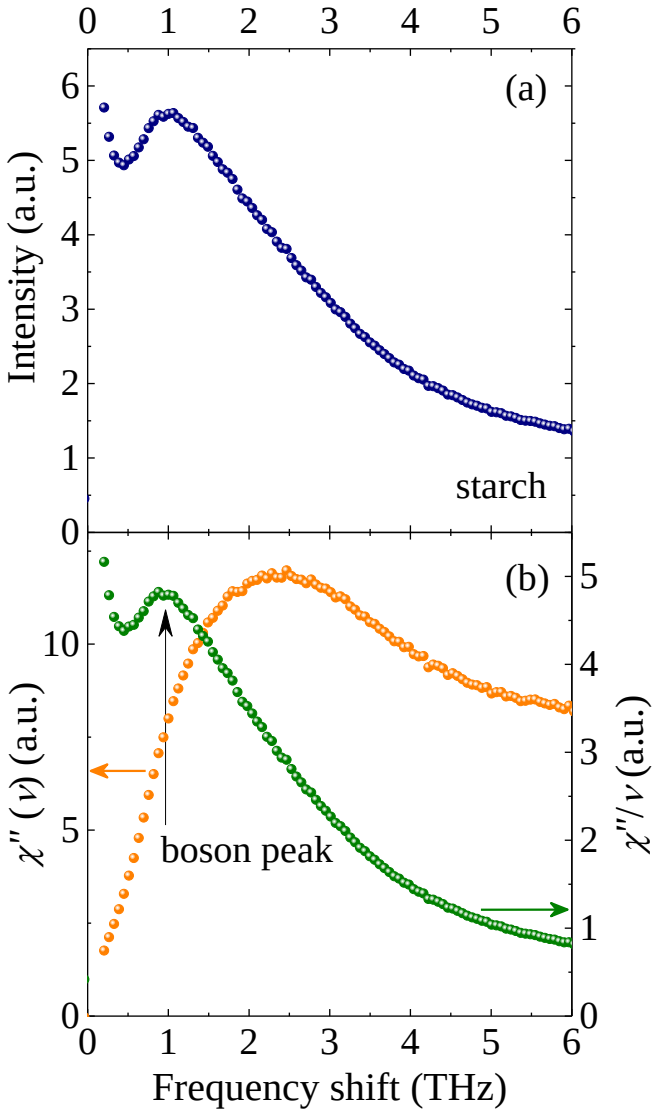
(a)
Intensity (a.u.)
starch
(b)
boson peak
χ'' (ν) (a.u.)
χ''/ν (a.u.)
Frequency shift (THz)